

Projected Changes in the Dynamics of Flood Hazard in the Grand River Basin, Canada

Abhishek Gaur^{1*} and Slobodan P. Simonovic¹

¹Department of Civil and Environmental Engineering, University of Western Ontario, London, Ontario, N6A 3K7, Canada.

Authors' contributions

This work was carried out in collaboration between both authors. Author AG designed the study, performed the statistical analysis, wrote the protocol, and wrote the first draft of the manuscript.

Author SPS assisted the study design, supervised the analyses, reviewed the first draft of the manuscript and helped with the revisions. Both authors read and approved the final manuscript.

Article Information

DOI: 10.9734/BJECC/2015/17705

Original Research Article

Received 26th January 2015
Accepted 13th April 2015
Published 17th April 2015

ABSTRACT

In this study future flooding frequencies have been estimated for the Grand River catchment located in south-western Ontario, Canada. Historical and future climatic projections made by fifteen Coupled Model Inter-comparison Project-3 climate models are bias-corrected and downscaled before they are used to obtain mid- and end of 21st century streamflow projections. By comparing the future projected and historically observed precipitation and temperature records it is found that the mean and extreme temperature events will intensify in future across the catchment. The increase is more drastic in the case of extreme events than the mean events. The sign of change in future precipitation is uncertain. Further flow extremes are expected to increase in magnitude and frequency in future across the catchment. The confidence in the projection is more for low return period (<10 years) extreme events than higher return period (10-100 years) events. It can be expected that increases in temperature will play a dominant role in increasing the magnitude of low return period flooding events while precipitation seems to play an important role in shaping the high return period events.

Keywords: Flooding; climate change; Grand River; Brantford.

*Corresponding author: Email: abhishek.gaur1988@gmail.com;

1. INTRODUCTION

Significant amount of changes in the climatic and flow patterns have been detected globally over the past few decades [1,2]. It is projected that the observed trends will continue and produce more drastic and unprecedented changes in the climatic and flow regimes in future. Many climate change impact assessment studies have been performed across Canada. Significant changes in key climatic variables [3,4,5,6] as well as flow magnitudes have been detected [7,8,9,10] in the past few decades.

The importance of analyzing and projecting extremes has been highlighted in [11]. It is now widely accepted that the frequency and magnitude of climatic and flow extremes will change significantly in future however the confidence associated with the sign and magnitude of change projected for future flooding frequencies is very low. The complex physical processes involved behind the generation of flow extremes make their future projections highly uncertain. Several studies have been performed in the past at local, regional and global scales that aim at estimating extreme flood magnitudes in future. For instance [12] utilized three different downscaling methodologies to estimate peak discharges of Rhine river basin in 2050 and concluded that the magnitude of peak discharges of 10 to 1250 year return period events can increase by 8%-17% in future. They found the use of weather generators and other downscaling tools helpful in generating long time-series of future rainfall and streamflow estimates. [13] performed a similar analysis on the river Meuse (France-Belgium) using projections from three Regional Climate Models (RCMs) and estimated end of 21st century flooding magnitudes. They identified the use of different Global Climate Models (GCMs) as a major source of uncertainty and recommended the usage of multiple GCMs while making future flow extreme estimates. [14] analyzed projections from three different climate models corresponding to emission scenario A2 and analysed climate change impact on flow regimes across Europe. They concluded that climate change may have region-specific impacts on flow patterns in the future and peak flow magnitudes will be altered mainly because of changing snow-melt dynamics owing to higher spring and winter-time temperatures. [15] analyzed projections from 11 GCMs and concluded that the global flow extremes are set to change in future though the extent of change varies spatially depending

on the flow generation mechanisms operating in different regions. Other studies [16,17,18,19] warrant similar findings of changing flood hazard and its dependence on regional flow generation process dominant in different regions across the globe.

A small number of climate change impact studies analyzing flow extremes have been performed in the southern Ontario region of Canada. [20] analyzed the impact of climate change on 10, 100 and 250 year return period flooding event magnitudes in the Upper Thames River Basin and concluded significant increases in flooding magnitudes over the 21st century. Up to 12% and 33% increases in flooding magnitudes were obtained for 100-year and 250-year return period flooding events by the end of the 21st century. [21] analyzed climate change impacts on flow extremes in the Spencer Creek watershed located near Hamilton, Ontario under the A2 scenario and concluded increases in their magnitudes in the 21st century. Overall a decreased annual runoff, increased winter and spring flows, lower summer and fall flows, and increased frequency of high flows is projected for the 21st century in this region [22].

In Ontario, Canada the most common time of flooding events is during the spring freshet and the most common mechanism of flooding is rain on snowmelt. Historically the biggest floods in Ontario have occurred following this mechanism. The second most common mechanism of flooding in Ontario is through heavy rainstorms [23]. In this paper future flood magnitudes and underlying mechanisms are explored for the Grand River catchment located in south-west Ontario, Canada. For doing so, changes in the magnitude and frequency of 2-year, 5-year, 10-year, 25-year and 100-year return period flow events are estimated for 2046-2065 (2050s) and 2081-2100 (2090s). To study the underlying flood generating mechanisms for future, changes in flooding magnitudes are studied separately for low (<10 years) and high (10-100 year) return period flooding events. To the best of our knowledge no study looking into flow extremes has been performed on this catchment before. A description of datasets, models used, study area and methodology followed in this research is provided in section 2 followed by presentation and discussion of results in section 3. The paper ends with a summary of conclusions made from this study.

2. DATA, MODELS, STUDY AREA AND METHODOLOGY

2.1 Datasets Used

Historical observed daily precipitation and temperature (maximum, minimum and mean) data for the period 1961-2000 are obtained from the National Climate Data and Information Archive (NCDIA) at 52 gauging stations located within the Grand River catchment. Gridded Global Climate Model (GCM) data provided by the Coupled Model Inter-comparison Project-Phase3 (CMIP3) of the World Climate Research Programme (WCRP) [24] have been used in this study. Daily precipitation, maximum temperature, minimum temperature and mean temperature data projected for historical (1961-2000) and future timelines (2050s and 2090s) are used. In this study 15 CMIP3 GCMs (listed in Table 1) have been selected based on the availability of consistent datasets in historical and future timelines and across the three emission scenarios: A1B, A2 and B1.

2.2 Hydrological Model Used

A semi-distributed hydrologic model WATFLOOD [25,26] is used to generate streamflow in the catchment. This model is based on the concept of Grouped Response Units (GRUs), where units

of similar hydrological response (or Hydrological Response Units) within the catchment are modelled together to calculate overland flow, interflow and base flow within the area of study. Overland flow or surface runoff in the WATFLOOD is generated by an infiltration excess which is defined using the Philip formula [27]. Overland flow is modelled using a simple storage-routing technique involving the Manning formulae. Interflow is calculated as a variable depth, shallow aquifer response defined as a linear relation with land surface and water content [28] while the base flow component is generated from a deep lower zone storage (LZS) reservoir which is fed by the upper zone storage (UZS) and generates outflow following a two parameter power law formulation. In this model GRUs are characterized based on surface land-cover. The parameters optimized in WATFLOOD are land-cover specific and are related to soil permeability, overland flow roughness, channel roughness, depression storage, and an upper zone depletion factor [26]. For generating streamflow event files are prepared for each time-step (monthly or yearly). Important model controls are specified in these event files. The event files for the period of study are run together to generate outflow. Streamflow calculation is performed for each GRU, the flow aggregated across all GRUs within a grid and routed downstream to the catchment outlet.

Table 1. Climate models considered in this study. Model outputs corresponding to the “Climate of the Twentieth Century” run and SRES scenarios A1B, A2 and B1 are included in the analysis

S. no	Model	Atmospheric component resolution	
		Horizontal (lat × lon)	Vertical (levels)
1	BCCR-BCM2.0, 2005	1.9° x 1.9°	L31
2	CGCM3.1(T47), 2005	2.8° x 2.8°	L31
3	CGCM3.1(T63), 2005	1.9° x 1.9°	L31
4	CNRM-CM3, 2004	1.9° x 1.9°	L45
5	CSIRO-MK3.0, 2001	1.9° x 1.9°	L18
6	CSIRO-MK3.5, 2005	1.9° x 1.9°	L18
7	GFDL-CM2.0, 2005	2.0°x 2.5°	L24
8	GFDL-CM2.1, 2005	2.0° x 2.5°	L24
9	GISS-ER, 2004	4° x 5°	L20
10	IAP-FGOALS, 2004	2.8° x 2.8°	L26
11	INGV-ECHAM4, 2005	1.9° x 1.9°	L18
12	IPSL-CM4, 2005	2.5° x 3.75°	L19
13	MIROC3.2(medres), 2004	2.8° x 2.8°	L20
14	MPI-ECHAM5, 2005	1.9° x 1.9°	L31
15	MRI-CGCM2.3.2, 2003	2.8° x 2.8°	L30

WATFLOOD has been used extensively for performing hydrological modelling across Canada [29,30,31] and is considered as a model capable of simulating important hydrological processes in large catchments [32]. In this study an extended version of the model: isoWATFLOOD model has been used. In the isoWATFLOOD model both the observed streamflow and river isotopes (δ_{18O}) levels are used as reference datasets to obtain more credible and physically representative model parameter sets. The benefit of this approach is that it reduces significantly the chances of equifinality in streamflow simulation and hence provides reliable estimates of surface, intermediate and baseflow components of the total flow. The model previously calibrated and validated on the Grand River has been used to estimate key hydrologic variables in the catchment. The details of hydrologic model calibration and validation process and related statistics are provided in [33,34,35]. In this study the calibrated isoWATFLOOD hydrologic model with 2x2 km² GRU scale is used directly to simulate future flows and no attempt to recalibrate the model has been made.

2.3 Study Area

The catchment selected for this study is the Grand River at Brantford. Grand River originates in the Dundalk and Grand valley region and flows 128 km southwards to drain into Lake Erie at Port Maitland. The Grand River catchment is the largest among south-western Ontario rivers encompassing around 6965 Km² of area and is home for more than 787,000 people [36]. Large urban centers such as Kitchener, Waterloo, Cambridge and Guelph are present in the central regions of the catchment. Remaining sections of the catchment are primarily dominated by agricultural land-cover which account for around 60-80% of the total area of the catchment [37].

Based on the geologic setting the Grand River watershed can be roughly classified into three sections of the upper, central and lower Grand watershed. Upper section is characterized by finer textured diamicton soils, less depression storage and large end-of-winter snowpacks which produces large amounts of overland runoff especially in the spring. The central region of the watershed has large areas of coarse-textured soils consisting of sand and gravel. This combined with hummocky moraine topography with closed depressions produces reduced overland runoff and high recharge to

groundwater, leading to sustained baseflow in main-stem tributary streams. The lower low-lying regions of the watershed consist primarily of clayey soil which generates high surface runoff and allows for low groundwater recharge. Catchment of Grand River at Brantford (Fig. 1) with an area of 5,210 km² roughly covers the upper and central Grand River watershed regions.

Temporal variations in precipitation, temperature and flow patterns are observed throughout the year. March to September months are the most rain-fed months of the year. Precipitation occurring within these months is found to be 20% higher than the monthly average while remaining months receive precipitation that is 30% lower than the monthly average. Significant temperature variability is observed with high summer average temperatures close to 20°C and low winter average temperatures around -7°C. Flow is regulated at several locations along the Grand River using seven dams: Luther, Conestogo, Woolwich, Laurel, Shand, Guelph and Shade's Mills Dam [38]. River discharge at Brantford varies across the year with high flows observed during the months of March and April and low flows are observed during the summer months. Further, relatively higher values of discharges are noted in all the winter months.

2.4 Methodology

2.4.1 Selection of climate model projections

A total of 41 climate model-scenario combinations as projected by the selected 15 GCMs corresponding to SRES scenarios: A1B, A2 and B1 are selected for analysis. The selection of these climate model-scenario combinations (out of a total of 45 scenarios) is made based on the availability of daily precipitation and temperature datasets required for the study.

2.4.2 Bias-correction of GCM data

Gridded climate model data are bias-corrected before it is used to generate future streamflow from the catchment. Statistical bias correction (SBC) approach outlined in [39] is used to perform bias correction of historical and future climate model data at 52 gauging stations across the catchment. In the SBC approach the raw climate model data are transformed so that the frequency histogram of corrected model baseline data (X_{cor}) matches with the intensity histogram

of observed data (X_{obs}) using transfer functions. Transfer functions for a particular climate variable are estimated by first calculating the cumulative distribution function (CDF) of the climate model data and the observed historical data and then by fitting transfer function equations between the two CDFs so that $CDF_{cor}(X_{cor}) = CDF_{obs}(X_{obs})$. Three sets of transfer function equations: linear, exponential and logarithmic have been introduced in [39] that can be used to bias-correct precipitation data. In this study, a combination of linear (equation 1) and exponential (equation 2) transfer functions to correct precipitation data. Further as recommended in [39] the bias correction of temperature data is performed on mean temperature, temperature range and skewness using linear transfer functions. Bias corrected estimates of temperature range and skewness are thereafter used to estimate maximum and minimum temperatures using equations 3 and 4. These sets of transfer functions have been recommended and used in many other climate change impact assessment studies [39,40].

Transfer functions obtained for historical timeline are thereafter used to bias-correct future precipitation and temperature data.

$$x_{bc} = a + bx \tag{1}$$

$$x_{bc} = (a + bx)(1 - e^{-(x-x_0)/\tau}) \tag{2}$$

$$t_{min}^{bc} = t_{mean}^{bc} - (t_{sk}^{bc} \times t_r^{bc}) \tag{3}$$

$$t_{max}^{bc} = t_{mean}^{bc} + t_r^{bc} \times (1 - t_{sk}^{bc}) \tag{4}$$

In the above equations a is the additive correction factor, b is the multiplicative correction factor, τ is the rate of approach of attaining the asymptote, x_0 is the dry day correction factor. Further t_{mean} , t_{sk} and t_r represents mean temperature, temperature skewness and temperature range respectively. Subscript/superscript bc denotes bias corrected data.

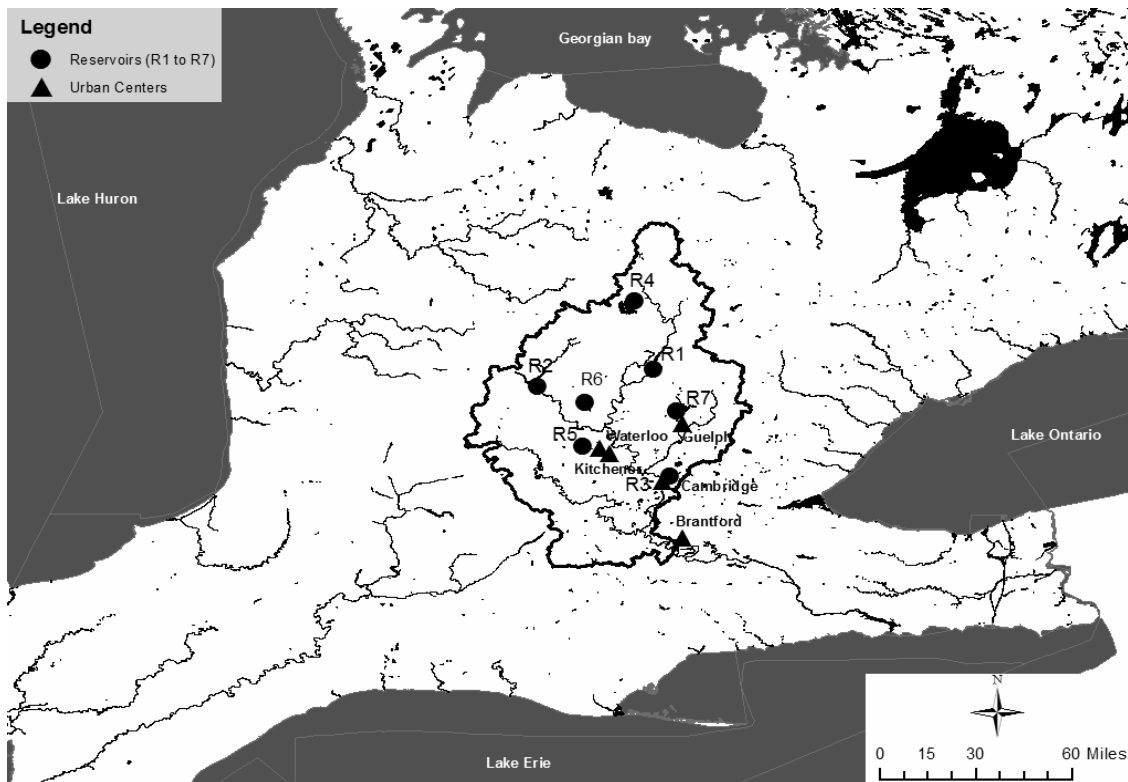


Fig. 1. Physiographic settings of the Grand River at Brantford. Major urban centres have been located within the catchment. The seven reservoirs located within the catchment: Shand, Conestogo, Shades, Luther, Laurel, Woolwich and Guelph are also denoted as R1 to R7 respectively

2.4.3 Downscaling of GCM data

Downscaling of bias-corrected climate data is performed using a weather generator approach. High resolution future climate data are produced by first producing scaled data from historical observed data using change factors. Distribution based change factors as outlined in [41] are calculated for each month using baseline (1961-2000) and future (2050s and 2090s) climate model data. A total of 100 bins are used to capture projected changes in the entire distribution of the climate data. Additive and multiplicative change factors are used for temperature and precipitation respectively. Generated future scaled data are used as input into a non-parametric, multisite multivariate weather generator model: MEBWG [42]. MEBWG first converts the climate data into independent components orthogonally, uses the Maximum Entropy Bootstrap procedure to generate synthetic replicates, and then transforms data back into original space by applying inverse orthogonal transformation. Twenty synthetic replicates of scaled data

corresponding to each GCM-scenario combination are produced and representative sets of precipitation-temperature combinations selected to encompass the precipitation-temperature range projected from weather generator outputs.

Scatter-plot based selection method as discussed in [43] is used to select representative precipitation-temperature combinations at each climate gauging station. In this study realizations projecting ‘minimum temperature-minimum precipitation’, ‘maximum temperature-maximum precipitation’ and ‘moderate temperature-moderate precipitation’ combinations in future are selected for analysis to encompass the range of climate variability imparted by the weather generator (as shown in Fig. 2). It can be pointed out that the selected realization results provide 120 years (40 years x 3 runs) of climate data corresponding to each GCM-scenario combination however it encompasses projected future climate uncertainty associated with 20 future realizations (equivalent to 40 years x 20 runs = 800 years) of data.

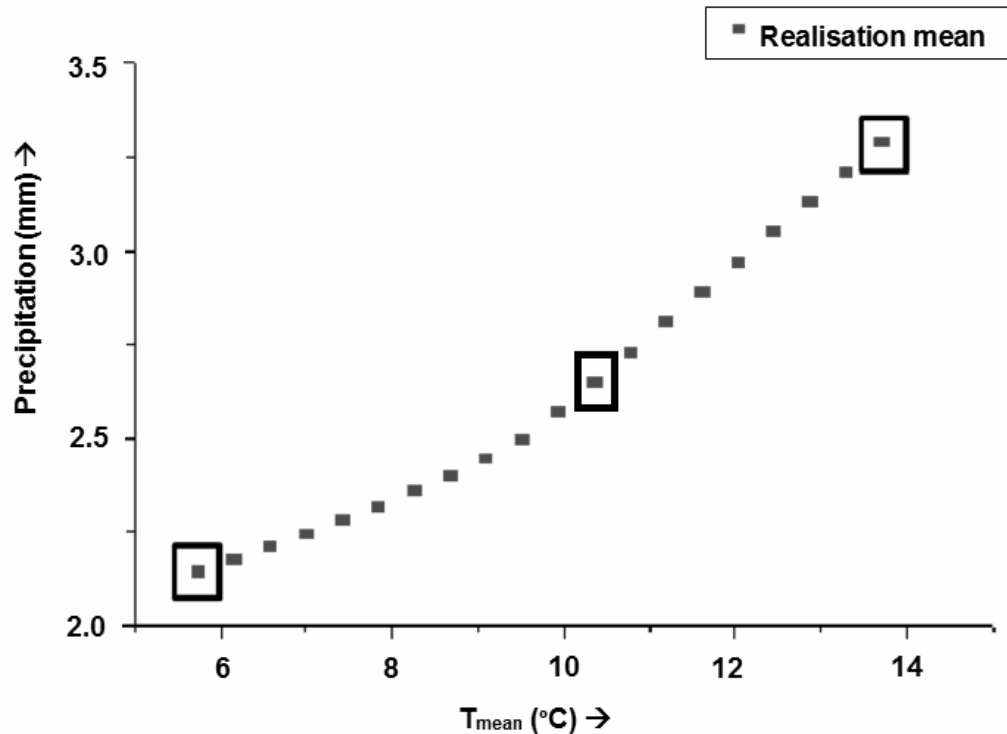


Fig. 2. Selection of representative precipitation-temperature combinations (within black boxes) from simulated future realisations at a gauging station: Appsmill

2.4.4 Generation and analysis of future streamflow projections

The isoWATFLOOD hydrologic model was used to streamflow in the catchment for future timelines. A streamflow series of 120 years is generated by combining flows obtained from the three representative precipitation-temperature combinations. For doing so the representative GCM outputs are first used to generate yearly event files for future timelines. The programs ragmet.exe and tmp.exe (part of the isoWATFLOOD model) are used to generate future gridded (2x2 km²) precipitation and temperature series across the catchment. The event files are chained together as continuous simulation and individual runs are performed for each individual representative scenario. Land-cover and reservoir release is assumed to be fixed to historical values while doing so. Historical observed and generated future flow-series are thereafter used to obtain flood magnitude and return period relationships. In this study, the Peak over Threshold (POT) method is employed to select flow peaks. Selection of independent peak flow values is made using the software WETSPRO [44]. The selection of independent flow peaks in WETSPRO is made using the following three criteria:

- Time between the two peaks should be greater than the recession constant k .
- Minimum discharge between the two peaks should be less than a fraction f of the peak discharge.
- Peak discharge should be greater than the threshold discharge value q_{lim} .

Values of parameters ' k ' and ' f ' are taken as 10 days and 0.37 respectively. These values of parameters have been recommended in [44] and have been used in previous studies [20]. Three peaks per year are selected (i.e. peak threshold is implicit) following the guidelines provided in [45,20]. Therefore 120 peaks flows were selected for the observed and each generated future flow series. The Generalised Pareto Distribution (GPD) has been recommended and used for fitting POT selected peaks in previous studies [20]. Selected flow peaks are therefore used to fit a GPD and associated parameters are estimated using the L-moments method. Flow quantiles corresponding to 2-year, 5-year, 10-year, 25-year, and 100-year return period floods are calculated. Return-period and flow quantile relationships are also established to compare the flood frequency distributions between historical and future timelines.

The return-period flow relationships obtained for each precipitation-temperature combination are related back to the GCM associated with it to explore the mechanism involved in their formation. Analysis is performed separately for low return period events (<10 years) and high return period events (10-100 years) to explore if the flood generating mechanisms will be different for small and large floods in future.

2.5 Limitations of the Methodology

It is worthwhile to point out that several improvements can be made in the current study to obtain more realistic future flooding projections. For instance in this study only the uncertainty associated with future climate projections has been encompassed while that associated with other steps i.e. use of different bias correction methodologies, downscaling methodologies and hydrologic models has been ignored. The array of future climate projections is expected to differ from that obtained in this study if other sources of uncertainty are included into the analysis process. Probable changes in future land-cover and reservoir operation rules can be also be incorporated to obtain more realistic future flow projections. Finally more recent climate model datasets provided in CMIP5 multi-model ensemble [46] can be used to improve the future flow projections presented in this study.

3. RESULTS AND DISCUSSION

The statistical bias correction approach is found to be effective in correcting bias associated with all moments of the GCM data. The effectiveness of this methodology is conveyed in Fig. 3 where a comparison between frequency histograms of raw and bias-corrected GCM data is made at a gauging station location. It can be seen that the overlap between observed and GCM data increased on bias-correction of precipitation as well as temperature data. Similar results are obtained for other GCMs considered in this analysis at different gauging stations across the Grand River catchment.

Significant changes in the precipitation and temperature regimes are projected across the catchment. In Table 3 the range of changes in precipitation and temperature means and extremes projected by all GCMs have been summarized. Data above 99th percentile are used to calculate extreme climate data statistics and changes are averaged over all 52 climate gauging stations located within the catchment. It

can be noted that an increase in the magnitude of mean and extreme temperature events is projected across the catchment. The range of changes projected for precipitation is very large and the sign of change is uncertain. It should

also noticed that the changes projected for precipitation and temperature extremes are significantly larger than those projected for means.

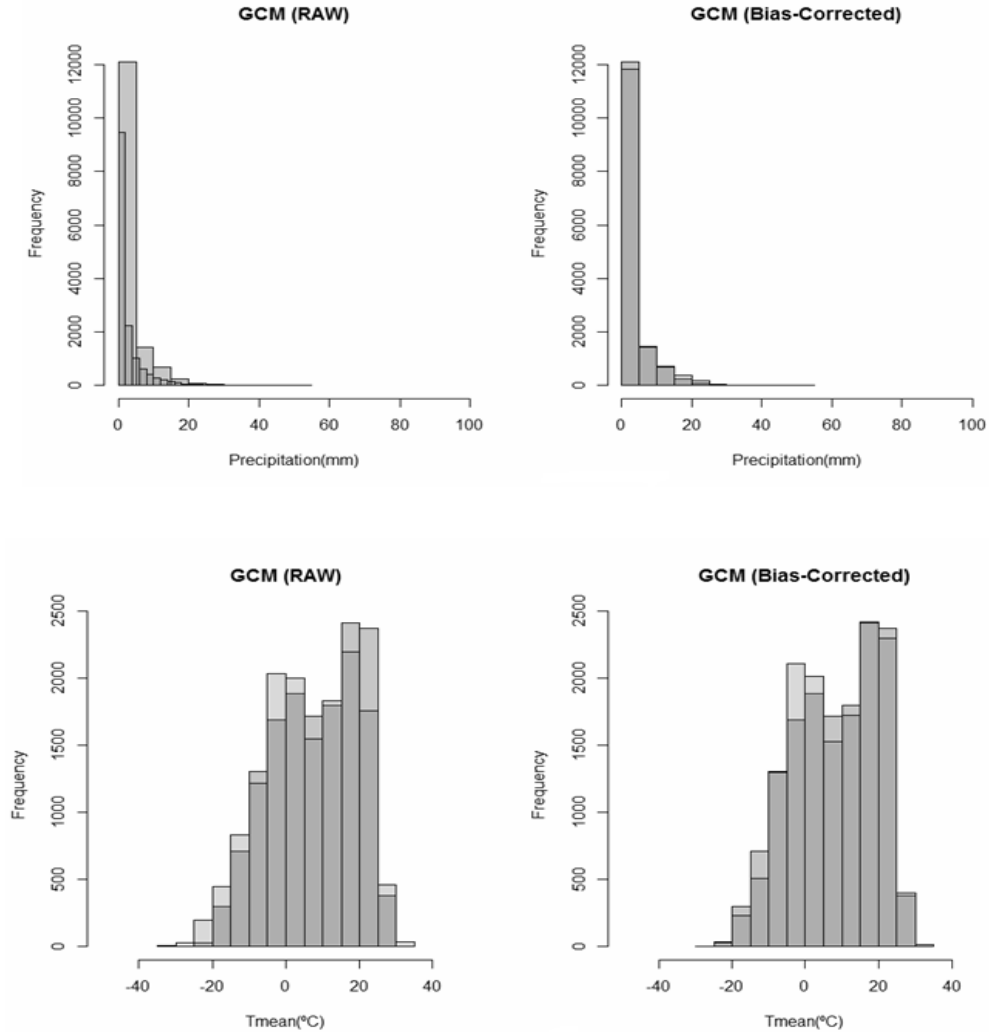


Fig. 3. Comparison of bin frequency distributions of observed, raw GCM and bias-corrected GCM (top) precipitation and (bottom) T_{mean} data at gauging station: Appsmill for GISS-AOM climate model (run1). Darker shade represents the overlap in bin frequencies between model and observed data

Table 2. Changes in mean and extreme precipitation and temperature projected for future across the Grand River catchment

Climate variable	Timeline	Change in mean	Change in extremes
Precipitation	2050s	-16.8% to +19.9%	-25.2% to +30.6%
	2090s	-12.8% to +26.8%	-33.1% to +33.7%
Temperature	2050s	+1.0°C to +5.2°C	+0.5°C to +6.6°C
	2090s	+1.4°C to +8.1°C	+1.9°C to +10.4°C

Subsequent changes in the extreme flow flow statistics are noticed at Brantford. The POT threshold values obtained with the implicit assumption were found to be significantly higher than those obtained for the historically observed data. The threshold values for all future scenarios are shown in Fig. 4. It should be noted that they are significantly higher for all the future GCM-scenario combinations considered for analysis than the historically observed value of 190 m³/s. This suggests that overall higher flows can be expected in future across the catchment.

Flow vs. cumulative probability and return period-flow plots for 2050s and 2090s are presented in Fig. 5. It can be noted that significant uncertainty is associated with the projected future flows. The changes in flooding magnitudes as projected for 2-year, 5-year, 10-year, 25-year and 100-year return period events are summarized in Table 3. It can be noted that the sign of change in flooding magnitudes is uncertain especially for floods with return periods between 10 and 100 years.

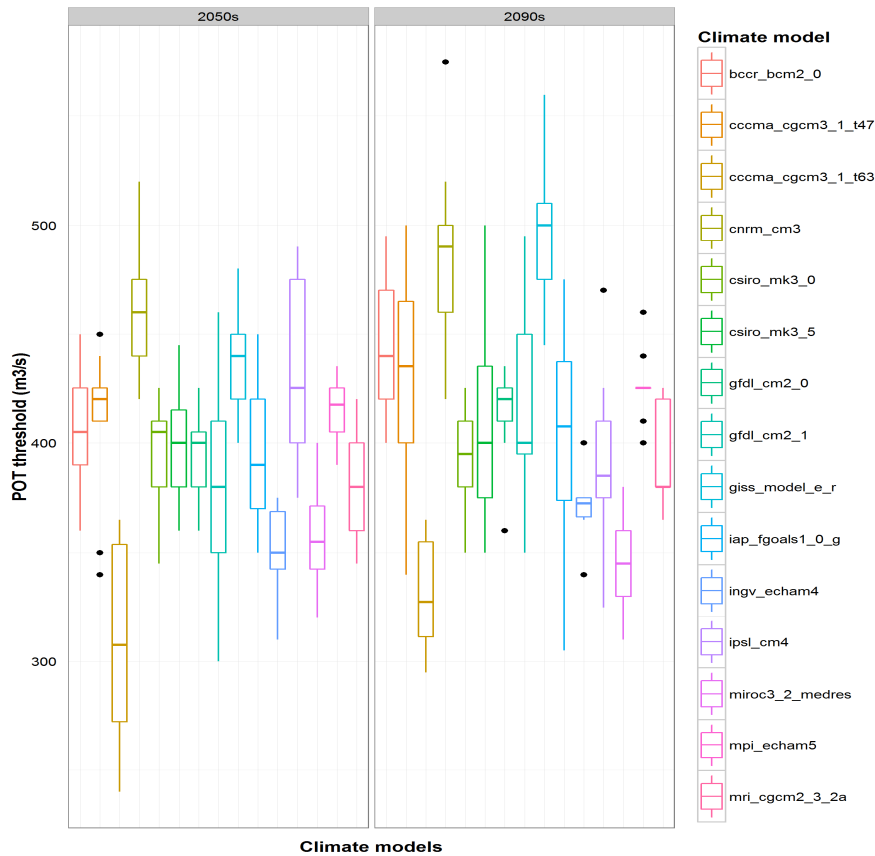


Fig. 4. POT threshold values obtained for each GCM-scenario combination considering the implicit assumption

Table 3. Percent change in flow quantiles of 2-year, 5-year, 10-year, 25-year and 100-year flooding magnitudes projected for 2050s and 2090s. The changes have been rounded off to the nearest whole numbers

Timeline	Degree of change	2-year	5-year	10-year	25-year	100-year
2050s	Max	87	43	32	24	27
	Min	17	3	-5	-15	-18
2090s	Max	95	59	46	35	35
	Min	24	5	-3	-13	-17

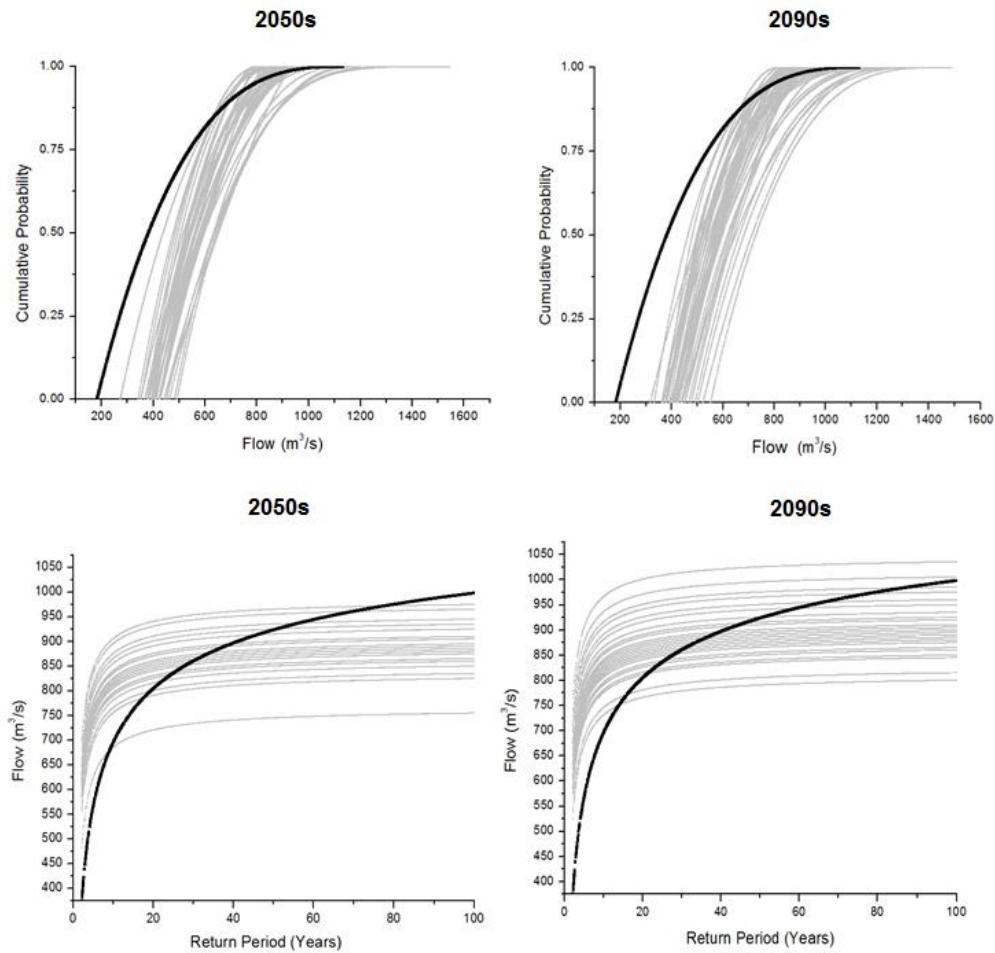


Fig. 5. Flow vs. cumulative probability (top) and return-period vs. flow (bottom) curves for projected future and historical observed flows at Brantford. Curves corresponding to specified future timelines are shown in grey shade while those corresponding to observed flows are shown in black

The sign of change projected by different scenarios is further explored. For doing so scenarios projecting more than +5% of changes in flooding magnitudes are deemed as projecting an increase in the future flooding magnitudes. Scenarios projecting less than -5% of changes in future are deemed as projecting decreases in the flooding magnitudes in future while those projecting changes between -5% to +5% are deemed as projecting no change in the flooding magnitudes in future. With this classification scheme it is found that for 2, 5 and 10 year return period flooding events an increase in future flooding magnitudes is projected by more than 50% of the scenarios. For 25 and 100 year return period events all three scenarios of change are equally possible because 50% concurrence is not achieved among analyzed

scenarios over the sign of change. Most scenarios analyzed for these higher return period events project either no change or even decreases in the flooding magnitudes. The results are summarized in Table 4 and the sign of change projected by at least 50% of the scenarios considered has been highlighted. These results suggest that higher flood magnitudes can be expected for low return period floods while the sign of change is uncertain for high return period events. Similarly by analyzing return-period vs. flow magnitude responses it can be suggested that the return period of smaller magnitude flooding events will decrease in future while the changes in return periods of higher magnitude flooding events are highly uncertain in future for flooding events with return period between 10 and 100 years.

To explore the reason behind this contrast in behavior of low and high return period events the obtained flood magnitudes are linked back to the changes in precipitation and temperature as projected by each GCM-scenario combination. The results are presented in Figs. 6 and 7 for low (<10 year) and high (10-100 year) return period events respectively. In the figures the location of each triangle corresponds to the precipitation and temperature change projected by each GCM scenario, color denotes the GCM associated, the shape signifies the increasing or decreasing flood magnitude trend and the size represents the magnitude of change in flooding frequency as projected by the model. It can be noticed that the flooding magnitudes of low return period events are projected to increase by all models regardless of the sign or magnitude of changes in precipitation projected by them. This suggests

that the increases in the magnitudes of low return period events are a result of higher catchment temperatures which leads to a higher snowmelt runoff and an increased flow in the catchment. On the other hand the magnitudes of high return period events are more uneven and are found to be largely controlled by increases in precipitation intensities as projected by the GCMs. This finding is robust as it is found that close to 90% (60%) of the GCM-scenario combinations which project an increase in the precipitation magnitudes by more than 10% (5%) project an increase in the magnitude of high return period flooding events. On the other hand, only 15% of the scenarios which project a decrease in future precipitation magnitudes, project an increase in the magnitude of high return period flooding events.

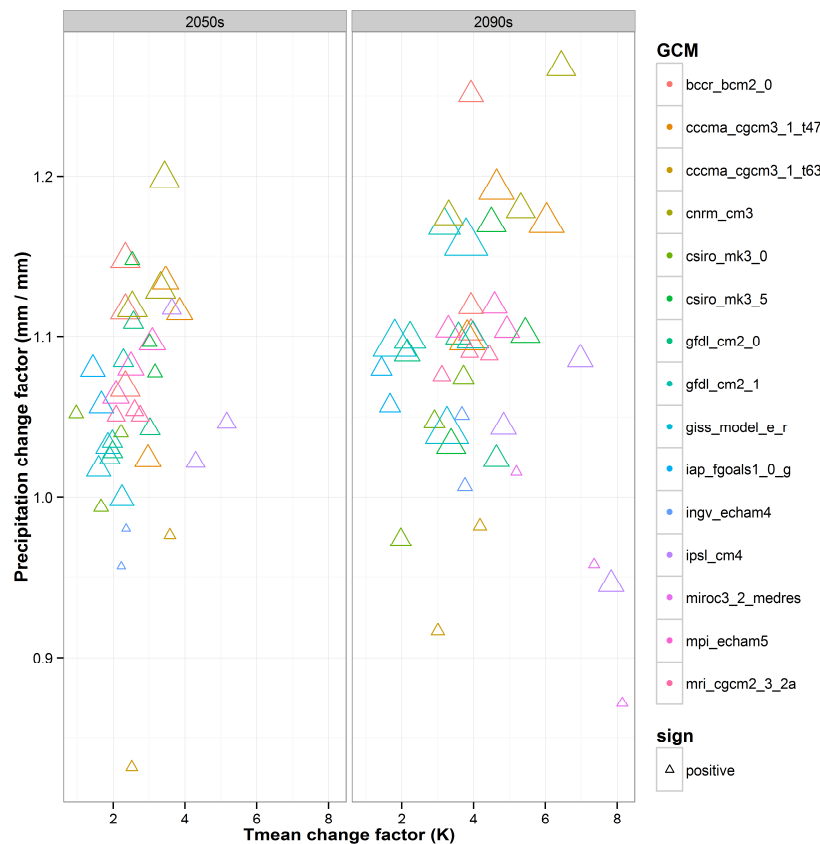


Fig. 6. Changes in the magnitude of flooding frequencies of small floods as projected by each GCM-scenario combination considered in the analysis. In the figure the location of each triangle corresponds to the precipitation and temperature change projected by each GCM scenario, color denotes the GCM associated, the shape signifies the increasing or decreasing flood magnitude trend and the size represents the magnitude of change in flooding frequency as projected by the model

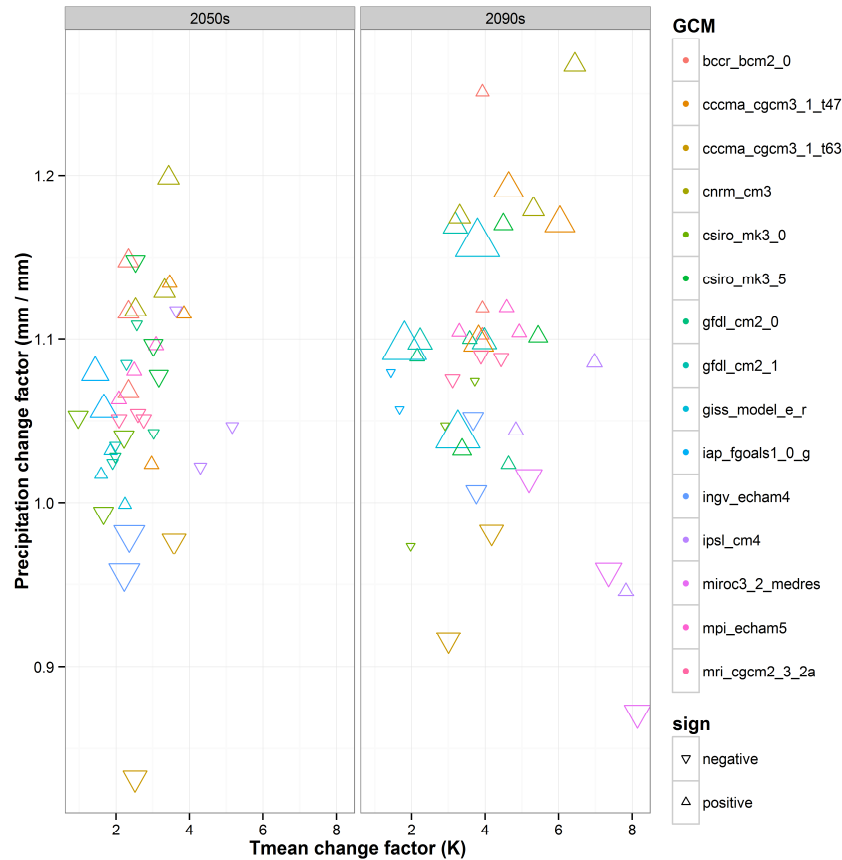


Fig. 7. Changes in the magnitude of flooding frequencies of large floods as projected by each GCM-scenario combination considered in the analysis. In the figure the location of each triangle corresponds to the precipitation and temperature change projected by each GCM scenario, color denotes the GCM associated, the shape signifies the increasing or decreasing flood magnitude trend and the size represents the magnitude of change in flooding frequency as projected by the model

Table 4. Percentage of total scenarios concurring over an increase, decrease or no change in future flooding magnitudes. The direction of change as projected by at least 50% of the scenarios is also highlighted for each future timeline

Timeline	Sign of change	2-year	5-year	10-year	25-year	100-year
2050s	Increase	100.0	97.5	72.5	22.5	17.5
	Decrease	0.0	0.0	2.5	32.5	47.5
	No change	0.0	2.5	25.0	45.0	35.0
2090s	Increase	100.0	100.0	73.8	35.7	31.0
	Decrease	0.0	0.0	0.0	28.6	33.3
	No change	0.0	0.0	26.2	35.7	35.7

This suggests that the anomalous changes in flooding frequencies of low and high return period events are led by the differences in dynamics involved in forming them. Historically high return period floods in Ontario have typically been formed following rain on snowmelt or

rainstorm mechanisms [23]. Figs. 6 and 7 suggest that this mechanism will most likely continue to form high return period extreme events in the catchment in future. Since large uncertainty is associated with the future precipitation magnitudes flooding magnitudes of

high return period events is also large unlike low return period events which convey a unanimous increase in flow magnitudes in future.

4. CONCLUSION

In this study possible impacts of climate change on future flooding magnitude and frequencies have been explored for a Canadian catchment: Grand River at Brantford. Selected catchment is typical of many industrialized, snow-fed catchments located across the globe and is characterized with diverse land-cover sections and regulated river systems. Using climate model projections from 15 CMIP3 climate models it has been found that the intensities of mean and extreme temperature events will increase in future across the catchment. Temperature intensities can increase by 1°C to 5°C by 2050s and by 2°C to 8°C by 2090s. The direction of change in the case of precipitation is more uncertain. The changes projected for precipitation intensities range from -17% to +20% by 2050s and between -13% to +27% by 2090s. Increases in the intensities of extreme events have been found to be more than the mean increases in intensities.

A wide range of changes in the flood magnitudes and frequencies are projected by climate models for future timelines at Brantford. From the analysis it seems highly probable that the magnitude of low (<10 year) return period flooding events will increase in future while the sign of change in the case of higher (10-100 year) return period flooding events is uncertain. It is found that the flooding magnitudes of 2-year (5-year) return period events will increase by 17% (3%) to 87% (43%) by 2050s and 24% (5%) to 95% (59%) by 2090s. It has been suggested here that a large uncertainty in high return period flooding events results from a high uncertainty in precipitation projections in the catchment. Precipitation plays an important role in forming high return period events in the catchment and therefore uncertainty in the precipitation magnitudes in turn imparts uncertainty in the magnitude of high return period flooding events. On the other hand low return period events are found to be dominated by effects of increases in temperatures projected across the catchment. The information about changes in flooding magnitudes of low and high return period events and their mechanisms of formation will be helpful to water resource managers in formulating appropriate flood mitigation measures within the Grand River basin.

ACKNOWLEDGEMENTS

The authors are thankful to Dr. Nicholas Kouwen for providing the calibrated isoWATFLOOD model for the Grand River catchment. We acknowledge the World Climate Research Programme's Working Group on Coupled Modeling for disseminating the CMIP3 model output. Further insightful comments provided by an anonymous reviewer and the editors on the original manuscript are also thankfully acknowledged.

COMPETING INTERESTS

Authors have declared that no competing interests exist.

REFERENCES

1. IPCC. Summary for Policymakers. In: Climate Change 2013: The Physical Science Basis. Contribution of Working Group I to the Fifth Assessment Report of the Intergovernmental Panel on Climate Change [Stocker TF, Qin D, Plattner GK, Tignor M, Allen SK, Boschung J, Nauels A, Xia Y, Bex V, Midgley PM, (eds)]. Cambridge University Press, Cambridge, United Kingdom and New York, NY, USA; 2013.
2. Intergovernmental Panel on Climate Change (IPCC). Climate Change 2007: The Physical Science Basis. Contribution of Working Group I to the Fourth Assessment Report of the Intergovernmental Panel on Climate Change [Solomon S, Qin D, Manning M, Chen Z, Marquis M, Averyt KB, Tignor M, Miller HL, (eds.)]. Cambridge University Press, Cambridge, United Kingdom and New York, NY, USA, 2007;996.
3. Zhang X, Vincent LA, Hogg WD, Niitsoo A. Temperature and precipitation trends in Canada during the 20th century. *Atmos Ocean*. 2000;38(3):395-429.
4. Shabbar A, Bonsal B. An assessment of changes in winter cold and warm spells over Canada. *Nat Hazards*. 2003;29(2): 173-188.
5. Bonsal BR, Zhang X, Vincent LA, Hogg WD. Characteristics of daily and extreme temperatures over Canada. *J Clim*. 2001; 14(9):1959-1976.
6. Vincent LA, Mekis E. Changes in daily and extreme temperature and precipitation

- indices for Canada over the twentieth century. *Atmos Ocean*. 2006;44(2):177-193.
7. Burn DH, Sharif M, Zhang K. Detection of trends in hydrological extremes for Canadian watersheds. *Hydrol Process*. 2010;24(13):1781-1790.
 8. Cunderlik JM, Ouarda TBMJ. Trends in the timing and magnitude of floods in Canada. *J Hydrol*. 2009;375(3-4):471-480.
 9. Dery SJ, Wood EF. Decreasing River Discharge in Northern Canada. *Geophys Res Lett*. 2005;32(10):L10401.
 10. Cunderlik JM, Simonovic SP. Hydrological extremes in a southwestern Ontario river watershed under future climate conditions. *Hydrol. Sci. J*. 2005;50(4):631-654.
 11. IPCC. Summary for Policymakers. In: *Managing the Risks of Extreme Events and Disasters to Advance Climate Change Adaptation* [Field CB, Barros V, Stocker TF, Qin D, Dokken DJ, Ebi KL, Mastrandrea MD, Mach KJ, Plattner GK, Allen SK, Tignor M, Midgley PM, (eds.)]. A Special Report of Working Groups I and II of the Intergovernmental Panel on Climate Change. Cambridge University Press, Cambridge, UK, and New York, NY, USA. 2012;1-19.
 12. Te Linde AH, Aerts JCJH, Bakker AMR, Kwadijk JCJ. Simulating low-probability peak discharges for the Rhine basin using resampled climate modeling data. *Water Resour. Res*. 2010;46:W03512.
 13. Leander R, Buishand TA. Resampling of regional climate model output for the simulation of extreme river flows. *J Hydr*. 2007;332(3-4):487-496.
 14. Schneider C, Laizé CLR, Acreman MC, Flörke M. How Will Climate Change Modify River Flow Regimes in Europe? *Hydrol Earth Syst Sc. Dis*. 2012;9(8):9193-9238.
 15. Hirabayashi Y, Mahendran R, Koirala S, Konoshima L, Yamazaki D, Watanabe S, et al. Global flood risk under climate change. *Nat Clim Chang*. 2013;3(9):816-821.
 16. Hirabayashi Y, Kanae S, Emori S, Oki T, Kimoto M. Global projections of changing risks of floods and droughts in a changing climate. *Hydrol. Sci. J*. 2008;53(4):754-772.
 17. Dankers R, Feyen L. Flood hazard in Europe in an ensemble of regional climate scenarios. *J Geophys Res*. 2009; 114(D16):D16108.
 18. Kingston DG, Taylor RG. Sources of uncertainty in climate change impacts on river discharge and groundwater in a headwater catchment of the Upper Nile Basin, Uganda. *Hydrol Earth Syst Sc*. 2010;14(7):1297-1308.
 19. Labat D, Godd Y, Probst JL, Guyot JL. Evidence for global runoff increase related to climate warming. *Adv Water Resour*. 2004;27(6):631-642.
 20. Das S, Simonovic SP. Assessment of uncertainty in flood flows under climate change impacts in the upper thames river basin, Canada. *Br. J. Hist. Sci*. 2012;2(4): 318-338.
 21. Grillakis MG, Koutroulis AG, Tsanis IK. Climate change impact on the hydrology of spencer creek watershed in Southern Ontario, Canada. *J Hydrol*. 2011;409:1-19.
 22. NRCan. *From Impacts to Adaptation: Canada in a Changing Climate*; 2008.
 23. ICLR. *Making Flood Insurable for Canadian Homeowners: A Discussion Paper*; 2010.
 24. Meehl GA, Covey C, Taylor KE, Delworth T, Stouffer RJ, Latif M, et al. The WCRP CMIP3 Multimodel Dataset: A New Era in Climate Change Research. *Bull. Amer. Meteor. Soc*. 2007;88(9):1383-1394.
 25. Kouwen N, Soulis ED, Pietroniro A, Donald J, Harrington RA. Grouped Response Units For Distributed Hydrological Modeling. *J Water Res Pl*. 1993;119(3): 289-305.
 26. Kouwen N. WATFLOOD/WATROUTE Hydrological Model routing & flood forecasting system. Unpublished manuscript [model user's manual]; 2007.
 27. Philip JR. An infiltration equation with physical significance. *Soil Sci*. 1954;77(1): 153-157.
 28. Snelgrove KR. Implications of lateral flow generation on land-surface scheme fluxes. Ph.D. Thesis, Department of Civil Engineering, University of Waterloo: Waterloo; 2002.
 29. Kouwen N, Danard M, Bingeman AK, Luo W, Seglenicks FR, Soulis ED. Case study: Watershed modeling with distributed weather model data. *Journal of Hydrologic Engineering*. 2005;10(1):23-38.
 30. Toth B, Pietroniro A, Conly FM, Kouwen N. Modelling climate change impacts in the peace and Athabasca catchment and delta: I—hydrological model application. *Hydrol Process*. 2006;20(19):4197-4214.

31. Pietroniro A, Fortin V, Kouwen N, Neal C, Turcotte R, Davison B, et al. Development of the MESH modelling system for hydrological ensemble forecasting of the Laurentian Great Lakes at the regional scale. *Hydrol Earth Syst Sc.* 2007;11(4):1279-1294.
32. Bingeman AK, Kouwen N, Soulis ED. Validation of the hydrological processes in a hydrological model. *J Hydraul Eng.* 2006;11(5):451-463.
33. Stadnyk T, Gibson J, Longstaffe F. Basin-Scale Assessment of Operational Base Flow Separation Methods. *J. Hydrol. Eng.* 2014;04014074.
34. Stadnyk-Falcone TA. Mesoscale hydrological model validation and verification using stable water isotopes: The isoWATFLOOD model. Ph.D. thesis, Univ. of Waterloo, ON, Canada; 2008.
35. Stadnyk TA, St. Amour NA, Kouwen N, Edwards TWD, Pietroniro A, Gibson JJ. A groundwater separation study in boreal wetland terrain: The WATFLOOD hydrological model compared with stable isotope tracers. *Isot. Environ. Health Stud.* 2005;41(1):49-68.
36. Grand River Conservation Authority (GRCA). Exploring Grand-Erie connections: Flow, quality and ecology. In 9th Annual Grand River Watershed Water Forum; 2009.
37. GRCA. Water Quality in the Grand River Watershed: Current Conditions and Trends (2003-2008); 2011.
38. GRCA. Grand River Conservation Authority 2005 Fall Report; 2005.
39. Piani C, Haerter JO, Coppola E. Statistical bias correction for daily precipitation in regional climate models over Europe. *Theor Appl Climatol.* 2009;99(1-2):187-192.
40. Rojas R, Feyen L, Dosio A, Bavera D. Improving pan-european hydrological simulation of extreme events through statistical bias correction of RCM-driven climate simulations. *Hydrol Earth Syst Sc. Dis.* 2011;8(2):3883-3936.
41. Anandhi A, Frei A, Pierson DC, Schneiderman EM, Zion MS, Lounsbury D, Matonse AH. Examination of change factor methodologies for climate change impact assessment. *Water Resour. Res.* 2011; 47(3):W03501.
42. Srivastav R, Simonovic SP. Multi-site, multivariate weather generator using maximum entropy bootstrap. *Clim Dyn;* 2014. DOI: 10.1007/s00382-014-2157-x.
43. Conservation Ontario. Guide for assessment of hydrologic effects of climate change in Ontario and Future Climate Change Datasets; 2011.
44. Willems P. A time series tool to support the multi-criteria performance evaluation of rainfall-runoff models. *Environ Modell Softw.* 2009;24(3):311-321.
45. Lang M, Ouarda TBMJ, Bobee B. Towards operational guidelines for over-threshold modeling. *J Hydr.* 1999;205:103-117.
46. Taylor KE, Stouffer RJ, Meehl GA. An Overview of CMIP5 and the Experiment Design. *Bull. Amer. Meteor. Soc.* 2012; 93:485-498.

© 2015 Gaur and Simonovic; This is an Open Access article distributed under the terms of the Creative Commons Attribution License (<http://creativecommons.org/licenses/by/4.0>), which permits unrestricted use, distribution, and reproduction in any medium, provided the original work is properly cited.

Peer-review history:

The peer review history for this paper can be accessed here:
<http://www.sciencedomain.org/review-history.php?iid=1109&id=10&aid=8858>